

# Dual Band-notched UWB MIMO Antenna with Uniform Rejection Performance

Jian-Feng Li\*, Duo-Long Wu, and Yan-Jie Wu

**Abstract**—A compact dual band-notched ultra-wideband (UWB) multiple-input multiple-output (MIMO) antenna with uniform rejection performance is designed on an FR4 substrate ( $35 \times 23 \times 1.6 \text{ mm}^3$ ). Compared with the existing UWB MIMO antennas, a second-order notched band with uniform performance for 5.15–5.825 GHz is achieved, which results from the interplay between a  $1/3\lambda$  open-end slot and a  $1/2\lambda$  parasitic strip. A  $1/4\lambda$  open-end slot is also applied to the 3.3–3.7 GHz reject band. The two slots are connected at their open ends, that can help to get the uniform reject performance for 5.15–5.825 GHz and make the high cutoff frequency of the impedance matching band go toward the higher frequencies. Excluding the two rejected bands, a band with  $|S_{11}| \leq -10 \text{ dB}$ ,  $|S_{21}| \leq -17 \text{ dB}$  and frequency ranged from 3.1 to 10.9 GHz is achieved, and results show that a uniform performance for 5.15–5.825 GHz is obtained.

## 1. INTRODUCTION

Making use of wide frequency to transmit signals, ultra-wideband (UWB) system has been reported to be resistant against frequency selective fading. UWB system suffers from multipath fading and should operate at extremely low spectral power level to avoid the interference from other systems. Thereby, its signal to noise ratio (SNR) is of a very low magnitude, the system performance deteriorated, and its development restrained. Meanwhile, without sacrificing transmitted power, multiple-input multiple-output (MIMO) technology has attracted major interest for its abilities to enhance the data rate and reliability in rich scattering environments [1]. Therefore, UWB MIMO technology is a rising research field to solve the multi-path fading and low SNR problems of UWB system [2] in recent years, and selective fading problem of MIMO system can also be improved by it.

To reduce the UWB antenna size or minimize the potential EM interferences between a UWB system and narrowband systems, various methods were used by the antennas [3–6]. However, high isolation UWB MIMO antenna with dual-notched band is difficult to obtain, especially for the second-order notched band with uniform performance, because the band-notched and decoupling structures may interrelate with each other, and unexpected destructive effect would be produced.

High isolation UWB MIMO antennas were designed in [7–10], but they did not offer band-rejection operation. The UWB MIMO antenna in [11, 12] rejected WLAN 5.5 GHz, and the high isolation UWB MIMO antenna obtained two rejection bands [13], but its notch-band-edge selectivity was poor. Due to four slot-type split ring resonators, a good notch-band-edge selectivity was obtained by the UWB MIMO antenna [14] with only one notched band. Thereby, it can be said that the design of high isolation dual band-notched UWB MIMO antenna with uniform rejection performance or good notch-band-edge selectivity is still a great challenge.

Based on our work in [15], a dual band-notched UWB MIMO antenna with uniform rejection performance for 5.15–5.825 GHz is proposed. A  $1/3\lambda$  open-end slot at about 5.7 GHz and a  $1/2\lambda$  parasitic

---

Received 16 December 2016, Accepted 24 January 2017, Scheduled 13 February 2017

\* Corresponding author: Jian-Feng Li (li.jf01@gdut.edu.cn).

The authors are with the Guangdong University of Technology, Guangzhou, Guangdong 510006, China.

strip at about 5.3 GHz are used for producing two notched bands, which are coupled to shape a single notched band with uniform rejection performance for 5.15–5.825 GHz. The reject band 3.3–3.7 GHz is also obtained by applying a  $1/4\lambda$  open-end slot. The two open-end slots are connected at their open ends, which is helpful for getting the uniform rejection performance and widening the operation band. With  $|S_{11}| \leq -10$  dB and  $|S_{21}| \leq -17$  dB, an operation band, ranging from 3.1 to 10.9 GHz excluding the two rejected bands, is achieved. Except for the two notched bands, the radiation efficiency  $\eta_{rad}$  higher than 60%, the ratio of mean effective gains (MEG) smaller than 1.0 dB, and the envelope correlation coefficient  $\rho_{eij} \leq 0.012$ .

## 2. ANTENNA CONFIGURATION

The geometry of the proposed UWB MIMO antenna consisting of symmetric antenna element 1 and 2 is illustrated in Fig. 1. With size of  $9 \times 16.5$  mm<sup>2</sup>, the antenna element is printed on the front side of an FR4 substrate with dimensions  $35 \times 23 \times 1.6$  mm<sup>3</sup> and relative permittivity  $\epsilon_r = 4.4$ . Two symmetric parasitic strips and the ground plane ( $gl = 6.3$  mm,  $gw = 35$  mm) are printed on the other side of the FR4 substrate, and the length of the parasitic strip is  $pl = 14.5$  mm, which is about  $1/2\lambda$  at 5.3 GHz. Two kinds of slots are etched into the ground plane. One with width of 0.4 mm is named slot 1\_1 or slot 1\_2, and the other with width of 0.3 mm is called slot 2\_1 or slot 2\_2. They are connected at their open ends. The length of slot 1\_1 is  $sl_1 = 12.5$  mm, while the length of slot 2\_1 is  $(sl_2 + sl_3) = 9$  mm.

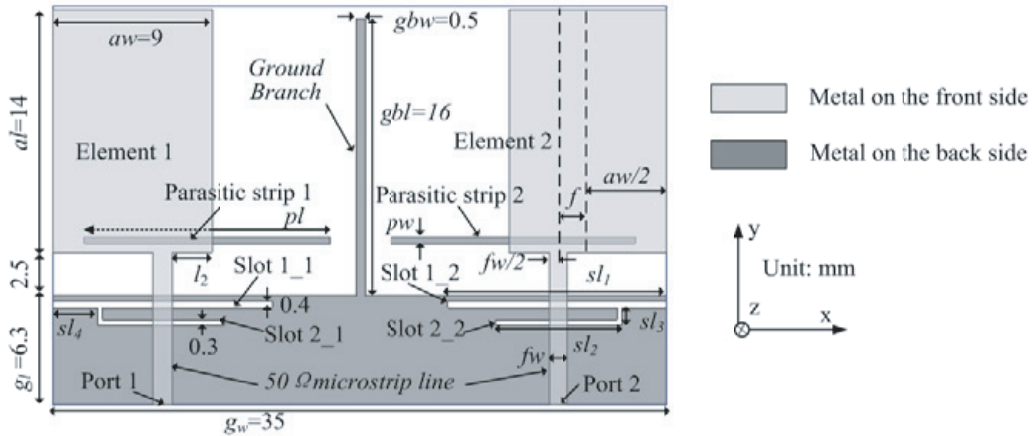


**Figure 1.** Structure of the proposed UWB MIMO antenna.

## 3. DESIGN PROCESS AND OPERATION MECHANISM

The proposed UWB MIMO antenna in Fig. 1 has been fabricated, and its photographs are shown in Fig. 2. The simulated and measured  $S$ -parameters are shown in Fig. 3. A  $|S_{11}| \leq -10$  dB and  $|S_{21}| \leq -17$  dB operation band of 3.1–10.9 GHz excluding the two rejected bands (3.3–3.7 GHz and 5.15–5.825 GHz) with a uniform reject performance for 5.15–5.825 GHz is achieved.

### 3.1. Discussion of Impedance Matching

A rectangular monopole antenna is usually applied to UWB operation band, such as antenna [16] and our design. The prototype of our design is MIMO antenna-I depicted in Fig. 4(a). The lower resonance frequency of a rectangular planar monopole can be approximately calculated by [16]:

$$f_{rL} = \frac{14.4}{a_l + g_l + h + r_1 + r_2} \text{ GHz} \quad (1)$$

$$\text{and } r_1 = \frac{a_l \times a_w}{2\pi(a_l + g_l + h)\sqrt{(1 + \epsilon_r)/2}}, \quad r_2 = \frac{g_l \times g_w}{2\pi(a_l + g_l + h)\sqrt{(1 + \epsilon_r)/2}} \quad (2)$$

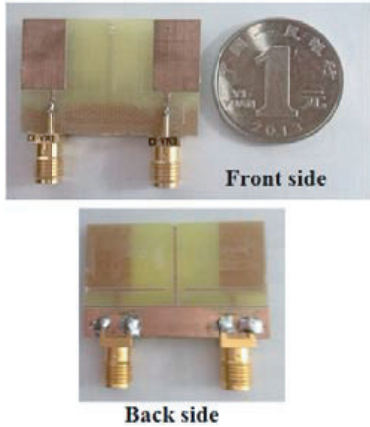


**Figure 2.** Photographs of the fabricated UWB MIMO antenna.

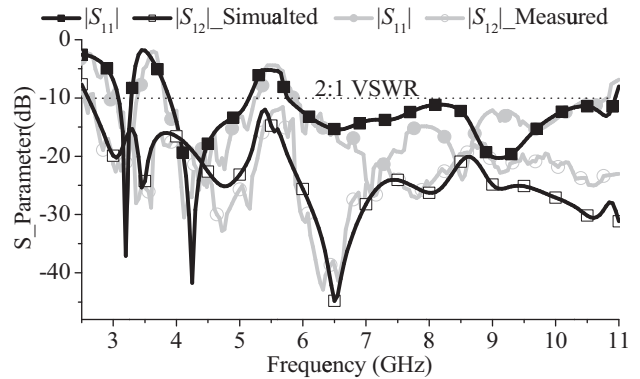


**Figure 3.** Measured and simulated  $S$ -parameters of the proposed UWB MIMO antenna.

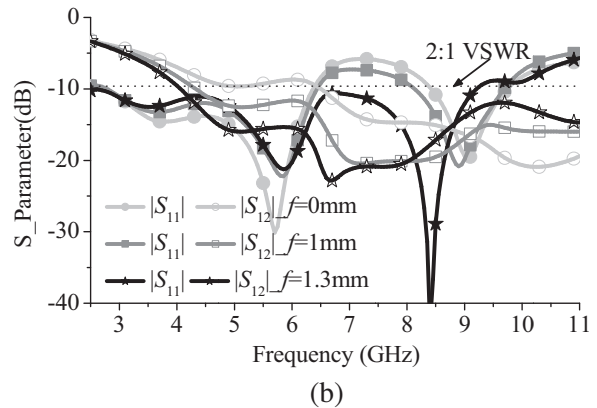
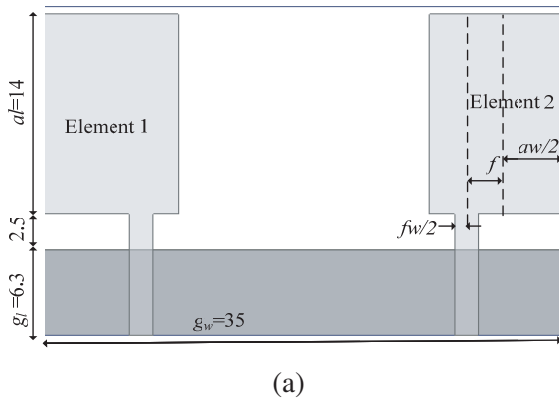


**Figure 4.** MIMO antenna-I: (a) configurations, (b)  $S$ -parameters.

where,  $a_l$ ,  $a_w$ ,  $g_l$ ,  $g_w$  and  $h$  are in centimeters, and they have the same values as the proposed antenna in Fig. 1. When  $f = 0$  mm, the calculated  $f_{rL}$  is 5.88 GHz according to Eqs. (1) and (2), and this result is in agreement with the simulated one in Fig. 4(b). The variation of  $f$  has great effect on current distributions, so  $|S_{11}|$  curve changes with varying  $f$ , especially for the frequencies at about 7.0 GHz, and then a desired performance is obtained for  $f = 1.3$  mm. But the upper frequencies of UWB band still cannot be covered.

### 3.2. Study of Notched Performance

For obtaining the reject band, two symmetrical open-end slots are etched into the ground plane of MIMO antenna-II shown in Fig. 5(a). The slot length is  $Sl$ , which can be calculated approximately by

$$Sl = \frac{C}{4f_0\sqrt{(1 + \epsilon_r)/2}} \quad (3)$$

Here,  $C$  is the speed of the light in free space, and the resonant frequency of the slot is denoted by  $f_0$ .  $f_0$  is 3.5 GHz for the reject band of 3.3–3.7 GHz, and  $Sl$  is 12.5 mm about  $1/4\lambda$  at 3.5 GHz according to Eq. (3). For the notched band of 5.15–5.825 GHz,  $f_0$  is 5.5 GHz, and  $Sl$  is 7.8 mm about  $1/4\lambda$  at 5.5 GHz. The application of the open-end slots makes the input impedance singular within their corresponding notched band, so the notched bands are obtained. Fig. 5(b) shows that the notched bands of 3.3–3.7 GHz and 5.15–5.825 GHz are obtained for  $Sl = 12.5$  mm and  $Sl = 7.8$  mm, respectively.

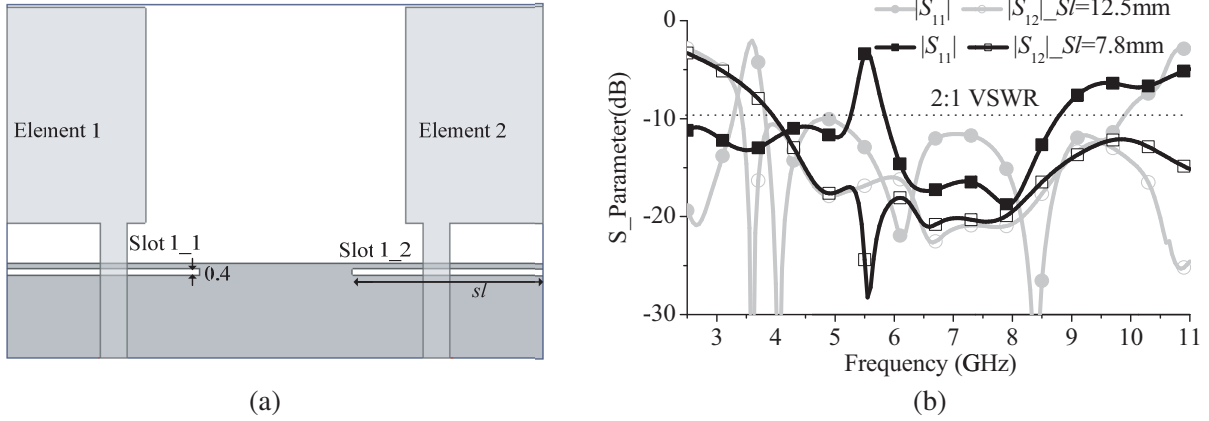


Figure 5. MIMO antenna-II: (a) configurations, (b)  $S$ -parameters with varying  $sl$ .

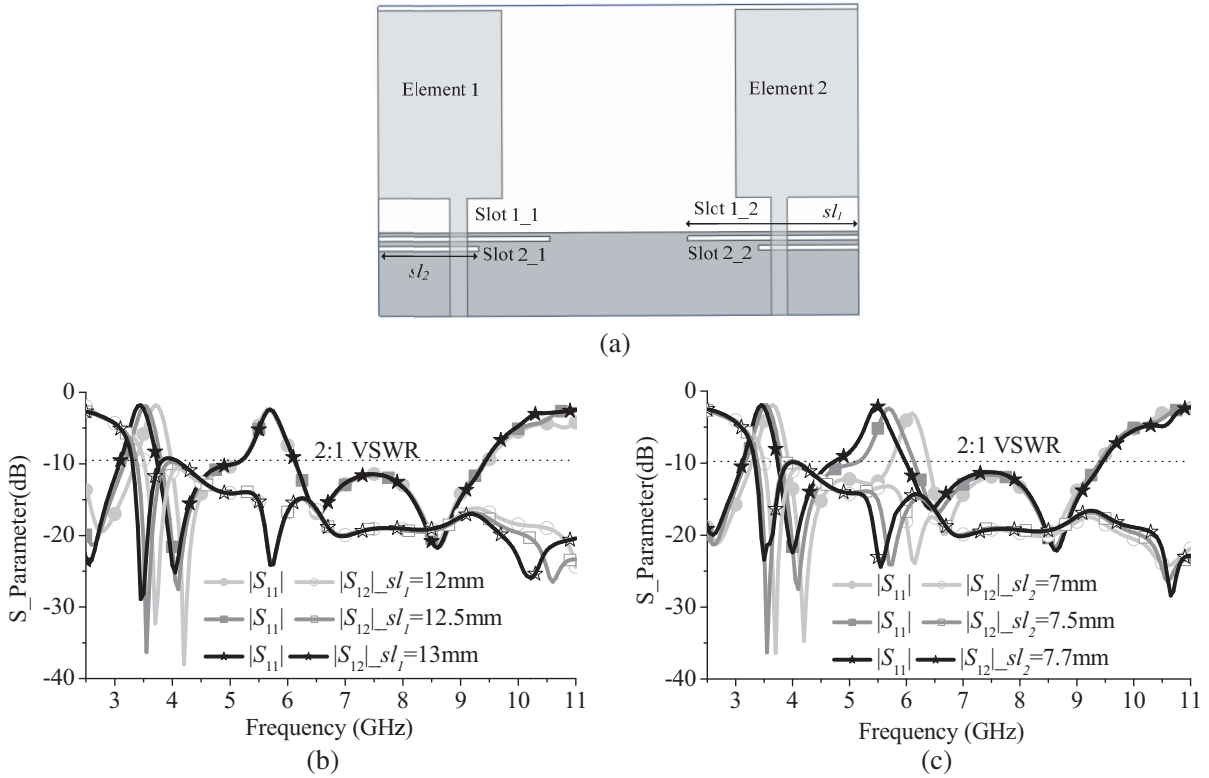


Figure 6. MIMO antenna-III: (a) configurations, (b)  $S$ -parameters with  $sl_1$ , and (c)  $S$ -parameters with  $sl_2$ .

In Fig. 6(a), two kinds of slots, respectively named slot 1-1 (or 2-1) and slot 2-1 (or 2-2), are applied by MIMO antenna III.  $sl_1$ , the length of slot 1-1, is 12.5 mm, and the length of slot 2-1 is  $sl_2 = 8.5$  mm. From Figs. 6(b) and (c), it is obvious that both the notched bands are achieved. Moreover, it can also be seen that 3.5 GHz notched band can be controlled effectively by  $sl_1$ , and the 5.5 GHz notched band goes toward the higher frequencies with the decrease of  $sl_2$ , but the effects of  $sl_1$  and  $sl_2$  on  $|S_{21}|$  curve are slight except the notched-band frequencies. Thus, we can say that the applications of slot 1-1 (1-2) and slot 2-1 (2-2) can control the bandwidth of their corresponding notched bands, respectively.

### 3.3. Uniform Rejection Performance and Improvement of the Operation Band

The dual band-notched filtering properties are achieved by MIMO antenna-III, but they both are first-order notched bands, and the uniform performance and notch-band-edge selectivity are bad. Moreover, the upper frequencies of UWB operation band still cannot be covered. Thus, antenna named MIMO antenna-IV is designed and displayed in Fig. 7(a). Note that there is no retuning work required for the previously determined dimensions, but slot 2-1 and slot 2-2 are redesigned. At their open end, slot 2-1 is connected with slot 1-1, and the length of slot 2-1 is  $(Sl_2 + Sl_3 + Sl_4) = 10$  mm, which is about  $1/3\lambda$  at 5.7 GHz. Slot 2-1 and slot 1-1 share one open end. Fig. 7(b) shows that the notched band produced by slot 2-1 becomes narrow, and the lower part of the 5.5 GHz notched band is no longer covered. However, the high cutoff frequency of  $|S_{11}|$  goes toward the higher frequencies to cover the whole UWB operation band. With redesign of the two slots, the current distribution of ground plane is changed, which can help the antenna element successfully excite a  $2\lambda$  resonant model at about 10.8 GHz.

In Fig. 8(a), two symmetrical parasitic strips with length of  $1/2\lambda$  at about 5.3 GHz are applied by the MIMO Antenna-V to regain the whole notched band of 5.15–5.5 GHz. We take Eq. (2) into account for obtaining the parasitic strips length at the very beginning of the design, and finally,  $(pl, pw) = (15$  mm, 0.5 mm). With element 1 excited while element 2 terminated with a  $50\Omega$  load, current distributions of MIMO antenna-V are displayed in Fig. 9. For the cases of 3.5 and 5.7 GHz, the currents mainly distribute around slot 1\_1 and slot 2\_1, respectively. The overlapping area between parasitic strip 1 and antenna element 1 can be considered as a capacitor, and some currents will be coupled to the parasitic strip 1 from the antenna element 1 through this capacitor, as shown in Fig. 9(b). Additional

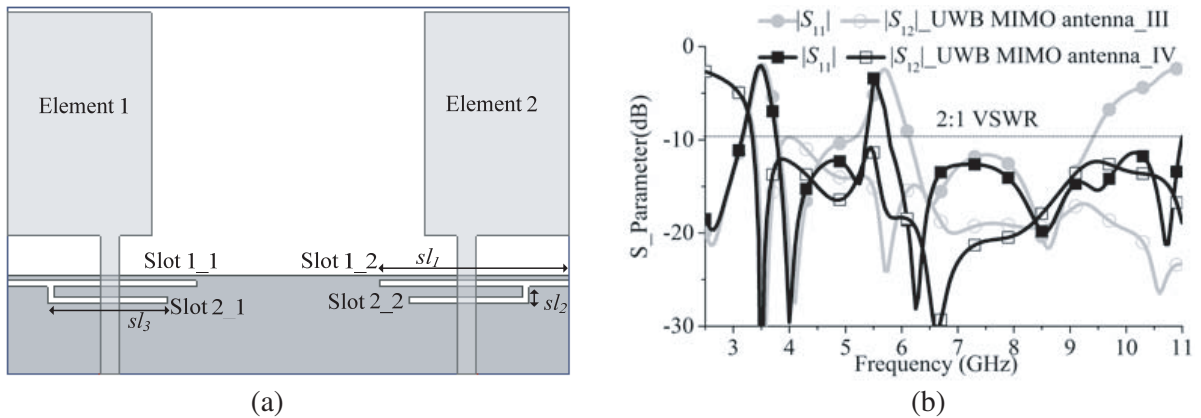


**Figure 7.** (a) Configurations of MIMO antenna IV, (b) comparison of  $S$ -parameters between MIMO antenna-III and MIMO antenna IV.

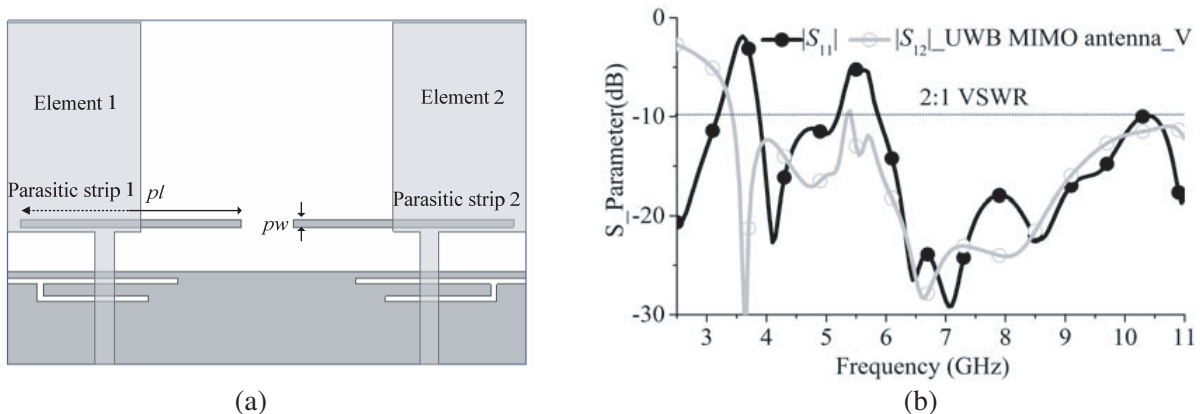


**Figure 8.** MIMO antenna V: (a) configurations, (b)  $S$ -parameters.

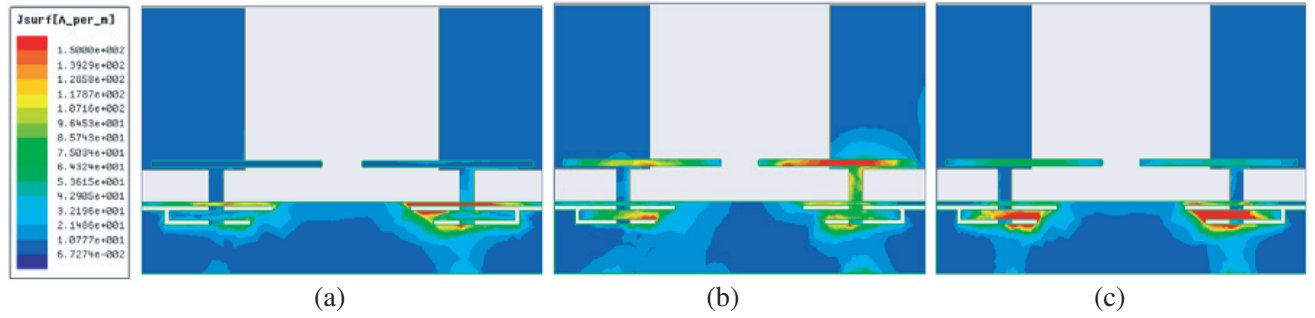


**Figure 9.** Current distributions of the MIMO antenna-V: (a)  $f = 3.5$  GHz, (b)  $f = 5.3$  GHz, and (c)  $f = 5.7$  GHz.

capacitive reactance is provided by this capacitor, and impedance matching of the antenna is destroyed for the frequencies about 5.3 GHz, thereby a notched band about 5.3 GHz is produced. Those two notched bands produced by slot 2-1 and parasitic strip 1 are coupled to shape a single notched band of 5.15–5.825 GHz with second-order characteristic. Fig. 8(b) shows that a uniform performance within this reject band is achieved. Moreover, two transmission poles at both sides of the notched band are produced, thus high notch-band-edge selectivity is obtained. A less-than-desirable performance is that some energy will be stored by this capacitor, and it will cause the peak levels of  $|S_{11}|$  and  $|S_{21}|$  for 5.15–5.825 GHz both getting a little lower with applying the parasitic strip, as shown in Fig. 8(b), but the result can still be considered acceptable for UWB MIMO application.

### 3.4. Improvement of Isolation and the Final Design

In Fig. 8(b), we can see that  $|S_{21}|$  is smaller than  $-15$  dB for most frequencies within UWB band, but it still needs to be improved for the frequencies at about 3.2 and 10.0 GHz. For our final design proposed in Fig. 1, a protruded ground branch is applied. Except for the two notched bands, isolation for the whole UWB operation band is improved ( $\geq 17$  dB), especially for the frequencies at about 3.2 and 10.0 GHz, as shown in Fig. 3. By comparing with the results in Fig. 8(b), we know the  $|S_{11}|$  curve and the two notched bands are almost unchanged for the application of the ground branch.

Table 1 represents the comparison of antenna characteristics, such as size and number of notched bands, and it can be seen that our design has good performance with compact size.

**Table 1.** Comparison of some parameters between three UWB MIMO antennas and the proposed antenna.

Parameter	Ref. [9]	Ref. [10]	Ref. [14]	Proposed Antenna
Active antenna element Area ( $\text{mm}^2$ )	240.25	742.5	81	126
Volume of Antenna ( $\text{mm}^3$ )	1280	4400	832	1288
Number of Notched Band	0	1	1	2
Isolation	$\geq 10$ dB	$\geq 17.2$ dB	$\geq 20$ dB	$\geq 17$ dB
Notch-Band-Edge Selectivity		Bad	Good	Good

## 4. DIVERSITY PERFORMANCE OF THE PROPOSED MIMO ANTENNA

With port 1 excited and port 2 terminated with a  $50 \Omega$  load, the normalized measured radiation patterns of the proposed antenna with the two kinds of slot, two parasitic strips and ground branches (shown in Fig. 1) at 3.2, 4.5 and 8.0 GHz are plotted in Fig. 10. The MIMO antenna has quasi-omnidirectional pattern in the  $H$ -plane ( $x$ - $z$  plane) and dipole-like pattern in the  $E$ -plane ( $y$ - $z$  plane), which is typical

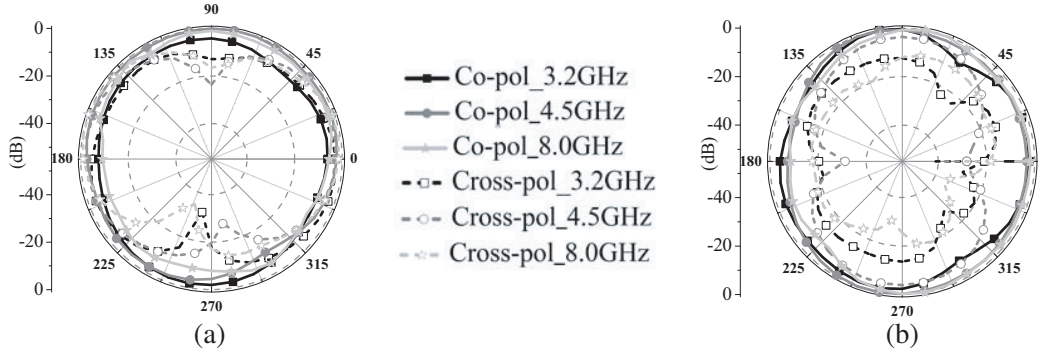


**Figure 10.** Measured radiation patterns of the proposed MIMO antenna. (a)  $x$ - $z$  plane, (b)  $y$ - $z$  plane.

for monopole antennas, and it will benefit the MEG for each antenna element.  $\eta_{rad}$  are given in Fig. 11, and the discrepancy of  $\eta_{rad}$  for the two antenna elements is small due to the symmetric placement and high isolation of the two elements.  $\eta_{rad} \geq 60\%$  both for the two elements, but sharply decreases and below 28% at the two notched bands, which demonstrates that our design has a good band-notched characteristic.

MEG ratios are used to quantify the power imbalance of the two antenna elements. Based on the assumptions of wireless environments [17] and measured data, the MEG ratios are calculated [18], and the comparison of the MEG ratios between the antennas [10, 13] and the presented antenna is listed in Table 2. We can see that the MEG ratios of our antenna is rather good. Except for the two reject bands, the maximum value of the MEG ratios is smaller than 1.0 dB, which satisfies one of the following criteria [19] used to guarantee good channel characteristics:

$$|MEG_i/MEG_j| \leq 3 \text{ dB}, \quad \rho_{eij} \ll 0.5 \quad (4)$$

where,  $i, j = 1, 2$ , which denotes the antenna elements 1 and 2, respectively.

**Table 2.** Comparison of ratio of MEGs between two UWB MIMO antennas and the proposed antenna.

Frequency (GHz)	Ref. [10]	Ref. [13]	Proposed Antenna
	$ MEG_i/MEG_j $	$ MEG_i/MEG_j $	$ MEG_i/MEG_j $
3.2	0.58 dB	0.65 dB	0.42 dB
4.5	1.05 dB	0.25 dB	0.23 dB
8.0	1.23 dB	0.26 dB	0.52 dB

The diversity performance of MIMO antenna is characterized in terms of envelope correlation coefficient (ECC)  $\rho_e$ , which can be derived from the  $S$ -parameters and  $\eta_{rad}$  in a uniform propagation environment [20]:

$$\rho_{eij} = \left| \frac{|S_{*ii} S_{ij} + S_{*ji} S_{jj}|}{|(1 - |S_{ii}|^2 - |S_{ji}|^2)(1 - |S_{jj}|^2 - |S_{ij}|^2)\eta_{radi}\eta_{radj}|^{1/2}} \right|^2 \quad (5)$$

It can be seen that small  $S$ -parameters and large  $\eta_{rad}$  can help to get the desired small  $\rho_e$ . Based on Eq. (5) and the measured data,  $\rho_e$  is calculated and shown in Fig. 12. Within the operation band,  $\rho_e < 0.015$  and satisfies the other criteria in Eq. (4), and another good metric is obtained for our designed.

According to the measured and calculated results, the proposed dual band-notched UWB MIMO antenna has high isolation and good uniform performance within the 5.5 GHz reject band.

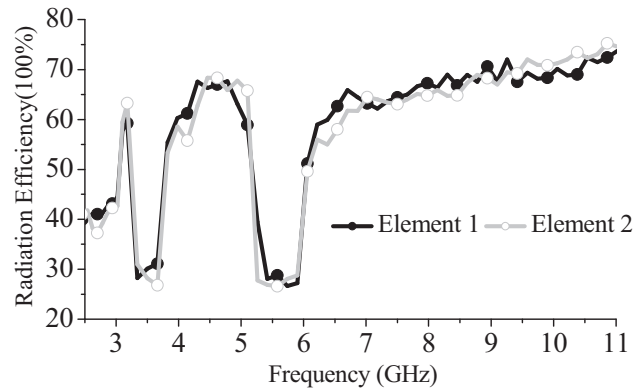


**Figure 11.** Radiation efficiencies of the antenna element.

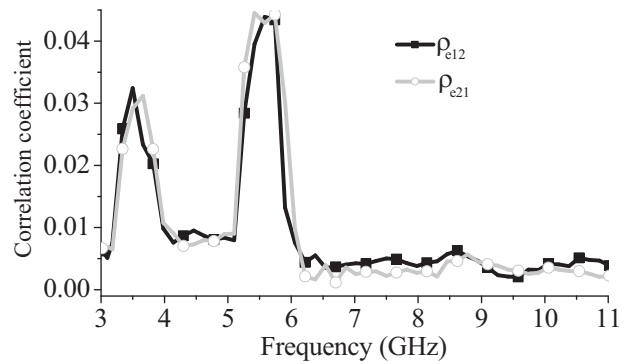


**Figure 12.** Correlation coefficient for the two elements of the proposed UWB MIMO antenna.

## 5. CONCLUSION

A compact dual band-notched UWB MIMO antenna has been presented and studied. Excluding the two rejected bands, the  $-10$  dB impedance bandwidth is 3.1 to 10.9 GHz, and the isolation is larger than 17 dB. One novelty of the design is the uniform performance for the reject band of 5.15–5.825 GHz, which is achieved for the second-order notched band. The other novelty is the two kinds of open-end slot connected at their open end to improve the impedance matching.

## ACKNOWLEDGMENT

This work is supported by Research on Compact Dual-Notch Band MIMO-UWB Antenna with High Isolation (15ZK0042), the Research Project of Guangdong Province (2013B090500035), and Science and Technology Program of Guangzhou (2014J4100202).

## REFERENCES

1. Bolin, T., A. Derneryd, G. Kristensson, V. Plicanic, and Z. Ying, "Two-antenna receive diversity performance in indoor environment," *IEEE Ele. Lett.*, Vol. 41, 1205–1206, 2005.
2. Ben Mabrouk, I., L. Talbi, M. Nedil, and K. Hettak, "MIMO-UWB channel characterization within an underground mine gallery," *IEEE Trans. Antennas Propag.*, Vol. 60, 4866–4874, 2012.
3. Saraswat, R. K. and M. Kumar, "Miniaturized slotted ground UWB antenna loaded with metamaterial for WLAN and WiMAX applications," *Progress In Electromagnetics Research B*, Vol. 65, 6580, 2016.
4. Ni, T., W.-M. Li, Y.-C. Jiao, L.-S. Ren and L. Han, "Novel compact UWB antenna with 3.5/5.5 GHz band-notched characteristics," *Journal of Electromagnetic Waves and Applications* Vol. 25, No. 16, 2212–2221, 2011.
5. Islam, M. T., R. Azim, and A. T. Mobashsher, "Triple band-notched planar UWB antenna using parasitic strips," *Progress In Electromagnetics Research*, Vol. 129, 161–179, 2012.
6. Chu, Q. X., C. X. Mao, and H. Zhu, "A compact notched band UWB slot antenna with sharp selectivity and controllable bandwidth," *IEEE Trans. Antennas Propag.*, Vol. 61, 3961–3966, 2013.
7. Yu, J. F., X. L. Liu, X.-W. Shi, and Z. Wang, "A compact four-element UWB MIMO antenna with Qsca implementation," *Progress In Electromagnetics Research Letters*, Vol. 50, 103–109, 2014.
8. Zhang, J. Y., F. Zhang, and W. P. Tian, "Compact 4-port ACS-fed UWB-MIMO antenna with shared radiators," *Progress In Electromagnetics Research Letters*, Vol. 55, 81–88, 2015.
9. Mao, C. X. and Q. X. Chu, "Compact co-radiator UWB-MIMO antenna with dual polarization," *IEEE Trans. Antennas Propag.*, Vol. 62, 4474–4480, 2011.

10. Toktas, A. and A. Akdagli, "Compact multiple-input multiple-output antenna with low correlation for ultra-wideband applications," *IET Micro. Antennas & Propag.*, Vol. 9, 822–829, 2015.
11. Lee, J. M., K. B. Kim, and H. K. Ryu, "A compact ultrawideband MIMO antenna with WLAN band-rejected operation for mobile devices," *IEEE Antennas Wirel. Propag. Lett.*, Vol. 11, 990–993, 2012.
12. Shrivishal, T., A. Mohan, and S. Yadav, "A compact Koch fractal UWB MIMO antenna with WLAN band-rejection," *IEEE Antennas Wirel. Propag. Lett.*, Vol. 14, 1565–1569, 2015.
13. Li, J. F., Q. X. Chu, and T. G. Huang, "Compact dual band-notched UWB MIMO antenna with high isolation," *IEEE Trans. Antennas Propag.*, Vol. 61, 4759–4766, 2013.
14. Xiao, R. J., X. B. Wei, and L. Jin, "A band-notched UWB MIMO antenna with high notch-band-edge selectivity," *Asia-Pacific Microwave Conference (APMC)*, Vol. 1, 1–3, 2015.
15. Li, J. F., D. L. Wu, Y. J. Wu, and G. Zhang, "Dual band-notched UWB MIMO antenna," *IEEE 4th Asia-Pacific Conf. Antennas and Propag. (APCAP)*, 25–26, 2015.
16. Thomas, K. G. and M. Sreenivasan, "A simple ultrawideband planar rectangular printed antenna with band dispensation," *IEEE Trans. Antennas Propag.*, Vol. 58, 27–34, 2010.
17. Ko, S. C. K. and R. D. Murch, "Compact integrated diversity antenna for wireless communications," *IEEE Trans. Antennas Propag.*, Vol. 49, 954–960, 2001.
18. Karaboikis, M., C. Soras, and G. Tsachtsiris, "Compact dual-printed inverted-F antenna diversity systems for portable wireless devices," *IEEE Antennas Wirel. Propag. Lett.*, Vol. 3, 9–14, 2004.
19. Karaboikis, M. P., V. C. Papamichael, G. F. Tsachtsiris, and V. T. Makios, "Integrating compact printed antennas onto small diversity/MIMO Terminals," *IEEE Trans. Antennas Propag.*, Vol. 56, 2067–2078, 2008.
20. Paul, H., "The significance of radiation efficiencies when using  $S$ -parameters to calculate the received signal correlation from two antennas," *IEEE Antennas Wirel. Propag. Lett.*, Vol. 4, 97–99, 2005.